

Dynamic Dark Energy Equation of State (EoS) and Hubble Constant analysis using type Ia supernovae from Union 2.1 dataset.

Syed Faisal ur Rahman^{1*}

¹ Institute of Space and Planetary Astrophysics (*ISPA*),
University of Karachi (*UoK*), Karachi, Pakistan

2019
September

Abstract

This paper constraints dynamic dark energy equation of state (EoS) parameters using the type Ia supernovae from Union 2.1 dataset. The paper also discusses the dependency of dynamic dark energy EoS parameters on the chosen or assumed value of the Hubble Constant. To understand the correlation between the Hubble Constant values and measured dynamic dark energy EoS parameters, we used recent surveys being done through various techniques such as cosmic microwave background studies, gravitational waves, baryonic acoustic oscillations and standard candles to set values for different Hubble Constant values as fixed parameters with CPL and WCDM models. Then we applied trust region reflective (TRF) and dog leg (dogbox) algorithms to fit dark energy density parameter and dynamic dark energy EoS parameters. We found a significant negative correlation between the fixed Hubble Constant parameter and measured EoS parameter, w_0 . Then we used two best fit Hubble Constant values (70 and 69.18474) $\text{km s}^{-1} \text{Mpc}^{-1}$ based on Chi-square test to test more dark energy EoS parameters like: JBP, BA, PADE-I, PADE-II, and LH4 models and compared the results with Λ -CDM with constant $w_{de} = -1$, WCDM and CPL models. We conclude that flat Λ -CDM and WCDM models clearly provide best results while using the BIC criteria as it severely pe-

nalizes the use of extra parameters. However, the dependency of EoS parameters on Hubble Constant value and the increasing tension in the measurement of Hubble Constant values using different techniques warrants further investigation into looking for optimal dynamic dark energy EoS models to optimally model the relation between the expansion rate and evolution of dark energy in our universe.

1 Introduction

The discovery of the accelerated expansion of the universe (**Riess et al. 1998** **Perlmutter 1999** **PerlmutterSchmidt 2003**) revolutionized modern cosmology and answered many questions related to the evolution of our universe. However, we are still trying to understand the ingredient which is likely responsible for the accelerated expansion of the universe i.e. dark energy. Dark energy seems to be something which is not only overcoming the tendency of collapse of the matter in our universe but it is also providing a push for the accelerated expansion of our universe (**Weinberg 2008**). After the discovery of the accelerated expansion of the universe in the late 1990s by HighZ Supernova and the Supernova Cosmology Project teams (**Riess et al. 1998** **Perlmutter 1999** **PerlmutterSchmidt 2003**) using the type Ia supernovae, several observations applying various signatures like cosmic microwave back-

*E-mail: faisalrahman36@hotmail.com

ground radiation (CMB), baryonic acoustic oscillation (BAO), Cepheid Variables, large scale structures etc. (Bennett et al. 2013)

Hinshaw et al. 2013 Planck 2018

Birrer et al. 2018 Macaulay et al. 2019 Riess et al. 2019), confirmed the accelerated expansion of our universe. Although, these observations confirm that our universe is going through a phase of accelerated expansion but these different observations also presented some serious problems by getting variations in their measurements of the cosmological parameters based on the standard model of cosmology or the Λ -CDM model (Liddle 2003 Jackson 2015 Rahman 2018) which is providing impetus towards the development of greater interest in non Λ -CDM model studies (Zhai et al. 2017 Khosravi et al. 2019 Sola et al. 2019). New standard candles like active galactic nuclei (AGN) are also being explored to get better measurements of cosmological parameters at high redshifts (Watson et al. 2011).

2 Cosmology from type Ia Supernova

Type Ia Supernovae are useful tools to be used as standard candles because of their almost standard absolute magnitude values. Therefore observations of apparent magnitude (m) and redshift (z) for type Ia Supernovae can lead to measurements of key cosmological parameters: $\Omega\Lambda$, Ω_r , and Ω_m , the dark energy, radiation and matter density parameters respectively within the Λ -CDM cosmology framework. The difference between apparent magnitude (m) and absolute magnitude is known as the distance modulus, μ :

$$\mu = m - M \quad (1)$$

Given a set of assumed cosmological parameters (C), the redshift of an object, its apparent magnitude and luminosity distance DL are linked thus:

$$m(C, z) = 5 \log(DL(C, z)) + M + 25 \quad (2)$$

Thus luminosity distance and distance modulus are

linked:

$$\mu(C, z) = 5 \log[DL(C, z)] + 25 \quad (3)$$

For a spatially flat universe, we can write luminosity distance as:

$$DL(z) = (1 + z)\chi(z) \quad (4)$$

Where,

$$\chi(z) = c\eta(z)$$

is the comoving distance and $\eta(z)$ is conformal loop back time which can be calculated as:

$$\eta(z) = \int_0^z \frac{dz'}{H(z')} \quad (5)$$

Here, $E(z) = \sqrt{\Omega\Lambda I(z) + \Omega_r(1+z)^2 + \Omega_m(1+z)^3}$ for flat Λ -CDM model. $I(z)$ depends on the parametrization of the dark energy equation of state (EoS) and for standard Λ -CDM model with EoS as $w_{de}(z) = -1$ (constant), the multiplier $I(z)$ becomes 1.

We can separate contribution of H_0 and absolute magnitude 'M' from the equations 2 and 3, as:

$$\tilde{M} = M + 25 + 5 \log(c/H_0) \quad (6)$$

Here 'c' is the speed of light in vacuum. This is often done to marginalize uncertainties arising from measurements of H_0 and M . However, the dominant contributor in these uncertainties is H_0 . We are fixing different H_0 s from various surveys to test them for most suitable H_0 for our dataset in relation with the equation of state (EoS) models in discussion which will minimize these uncertainties for the most suitable value of H_0 . Therefore instead of separating \tilde{M} , we can fit cosmologies using the equations 2 and 3. The contribution from absolute magnitude uncertainties is very minor if we apply proper fits for coefficients for stretch, color and probability of supernova in data are hosted by galaxies with less than certain threshold mass. We use Union 2.1's compilation Suzuki et al. 2012 magnitude vs redshift table which used fitted values for coefficients of stretch, color and the probability that a particular supernova in dataset was hosted by a low-mass galaxy. The

dataset also employs a constant $M \approx -19.31$ with uncertainties in distance modulus arising from fitting values and systematic contributions mentioned separately as distance modulus error which we incorporated in our model fitting using TRF and dogbox (VoglislLagaris 2004) and χ^2 analysis, and so it is absorbed in the parameter error bounds provided H0 is set to an optimal value.

3 Dataset and Data Analysis Techniques

For our study, we use Union 2.1 (Suzuki et al. 2012) dataset publicly shared by Supernova Cosmology Project (SCP) (Perlmutter 1999 PerlmutterSchmidt 2003Amanullah et al. 2010). The dataset is comprised of 580 type Ia supernovae which passed the usability cuts. The dataset is comprised of redshift range $0.015 \leq z \leq 1.414$ with median redshift at $z \approx 0.294$.

We use SciPy's (Jones et al. 2001) optimize package's trust region reflective (TRF) and dog leg (dogbox) algorithms (VoglislLagaris 2004), which are suitable for problems with constraints as in our case, to fit dark energy density parameter and dynamic dark energy EoS parameters for Λ -CDM, WCDM, CPL, JBP, BA, PADE-I, PADE-II and LH4 models (BarbozaAlcaniz 2008ChevallierPolarski 2001Linder 2003 Jassal et al. 2005aJassal et al. 2005b LinderHuterer 2005 Wei et al. 2014). We also apply grid method to obtain maximum likelihood (DavisParkinson 2016) for WCDM and CPL to compare results obtained through TRF and dog leg methods (VoglislLagaris 2004). We used TRF and dogbox options simultaneously with our selected models and then used the best fit results based on the χ^2 values.

4 Dynamic Dark Energy Equation of State (EoS)

$$I(z) = \exp(3 \int_0^z \frac{1 + w_{de}(z')}{1 + z'} dz') \quad (7)$$

In order to extend the standard Lambda-CDM model to incorporate dynamic dark energy EoS, we can define $I(z)$ as:

For the study we tested various dynamic dark energy EoS models.

We started with standard flat Lambda-CDM model with $w_{de} = -1$ and then tested WCDM model by treating w_{de} as free parameter. Then we moved towards more complex CPL, JBP, BA, PADE-I, PADE-II and LH4 models (BarbozaAlcaniz 2008ChevallierPolarski 2001Linder 2003 Jassal et al. 2005aJassal et al. 2005b LinderHuterer 2005 Wei et al. 2014) with model equations as:

CPL (ChevallierPolarski 2001 Linder 2003)

$$w_{de}(z) = w_0 + w_a \frac{z}{(1+z)} \quad (8)$$

JBP (Jassal et al. 2005aJassal et al. 2005b)

$$w_{de}(z) = w_0 + w_a \frac{z}{(1+z)^2} \quad (9)$$

BA (BarbozaAlcaniz 2008)

$$w_{de}(z) = w_0 + w_a \frac{z(1+z)}{(1+z^2)} \quad (10)$$

PADE-I (Wei et al. 2014)

$$w_{de}(z) = \frac{w_0 + w_a \frac{z}{(1+z)}}{1 + w_b \frac{z}{(1+z)}} \quad (11)$$

For $w_b = 0$, PADE-I reduces to CPL model.

PADE-II (Wei et al. 2014)

$$w_{de}(z) = \frac{w_0 + w_a \ln(\frac{1}{1+z})}{1 + w_b \ln(\frac{1}{1+z})} \quad (12)$$

Linder-Huterer (LH4) (**LinderHuterer 2005**)

$$w_{de}(z) = w_0 + \frac{(w_a - w_0)}{1 + \frac{1}{(1+z)^{a_t}}^{1/T}} \quad (13)$$

For parameter boundaries for TRF and dog leg analysis, we set $\Omega\Lambda$ boundary between 0.65 and 0.75. For w_0 , we set the upper boundary as $w_0 < -1/3$ which is a pre-condition for accelerated expansion of our universe but for lower limits we first set restrict it to $w_0 \geq -1$ to exclude phantom dark energy (**Vikman 2005Farnes 2018**) and keeping it in quintessence regime (**Weinberg 2008**). Then we set as $-\infty < w_0 \leq -1/3$ to allow phantom dark energy. This was done to minimize boundary condition bias while running the optimization algorithms. Similarly for w_a , we chose two set of boundaries $-5 \leq w_a \leq 5$ and $-0.3 \leq w_a \leq 0.3$ to avoid localization bias for optimization algorithm. In case of PADE I and II, w_b boundaries are set as $-1 < w_b < 0$ while others remain same. In LH4 case, we set both T and a_t between 0 and 1.

5 Hubble Constant Value

The value of Hubble Constant has recently been a topic of great interest in physics and astronomy community. It had been studied in the past like the first precise measurements by Sandage 1958 (**Sandage 1958**) which gave $H_0=75$ but recent interest has increased as the measurements of H_0 from cosmic microwave background (CMB), baryon acoustic oscillations (BAO), standard candles and others do not seem to agree with each other (**Freedman 2017Jackson 2015 Planck 2018 WojtakAdriano 2019Vattis et al. 2019Riess et al. 2019**). This problem has become even more interesting as the expansion rate is found to be same in all directions by Soltis et al. 2019 based on 1000 type Ia supernovae sample. (**Soltis et al. 2019**) Therefore we considered it appropriate to measure CPL and Λ CDM model parameters by fixing H_0 values from Planck 2018, Riess 2018, Abbott et al. 2017, Planck+SNe+BAO-Planck 2018,

Planck+BAO/RSD+WL-Planck 2018, H0LiCOW 2018 and DES 2018 (**Abbott et al. 2017 Birrer et al. 2018**). We also fit our own value for Union 2.1 dataset (**Suzuki et al. 2012**) using the kinematic expression from Riess et al. 2016 (**Riess et al. 2016**) for luminosity distance with source redshift of $z < 0.04$. Figure 1 shows that luminosity distances from (14) is in good agreement with luminosity distances from (4) for $z < 0.04$ using various EoS models.

The kinematic expression from Riess et al. 2016 is written as:

$$DL(z) = \frac{cz}{H_0} \left[1 + \frac{(1-q_0)z}{2} - \frac{(1-q_0-3q_0^2+j_0)z^2}{6} + O(z^3) \right] \quad (14)$$

With $q_0 = -0.55$ and $j_0 = 1$.

We can see from tables 1 and 2 that our best measurements based on χ^2 values for both CPL and Λ CDM are obtained through $H_0=70 \text{ km s}^{-1} \text{ Mpc}^{-1}$ which is measured by Abbott et al. 2017 by studying gravitational waves (GW170817) (**LIGO 2017Abbott et al. 2016Abbott et al. 2017**) from neutron stars collision and was also measured by Wilkinson Microwave Anisotropy Probe (WMAP) (**Bennett et al. 2013**) with WMAP only dataset. Our second best measurements were obtained through the best fit $H_0=69.18473827 \hat{A} 0.50179901$ or approximately $69.185 \text{ km s}^{-1} \text{ Mpc}^{-1}$ value from Union 2.1 dataset using kinematic expression for luminosity distance which is closer to the value obtained by (**Bennett et al. 2013**) using WMAP+eCMB+BAO+ H_0 data set (**Hinshaw et al. 2013**). We applied TRF with bounds $65 \leq H_0 \leq 75$ to obtain the best fit H_0 value. (**Bo 2019**). These values are interestingly somewhat in the middle region of the H_0 values obtained by early universe studies (**GorbunovRubakov 2011**) like Planck cosmic microwave background (CMB) (**Planck 2014aPlanck 2014bPlanck 2016Planck 2018**) or baryon acoustic oscillations (BAO) (**Grieb et al. 2017Macaulay et al. 2019**) which give $H_0 \approx 67$ and standard candles studies like (**Riess et al. 1998**

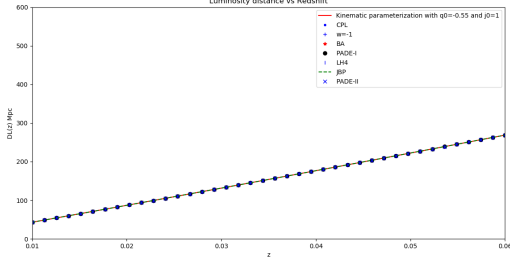


Figure 1: Luminosity distance plots using kinematic expression for $DL(z)$ and comparison with $DL(z)$ using various EoS models and Λ -CDM with $w_{de}(z)$ as a constant value of $w=-1$.

Riess et al. 2007 Riess et al. 2016
Riess et al. 2018a Riess et al. 2018b
Pietrzynski et al. 2019 Riess et al. 2019)
which give $H_0 > 73$. Because of this discrepancy in the measurement of H_0 , higher redshift studies of type Ia supernovae and other standard candles are becoming important (Risaliti Lusso 2019 Riess et al. 2018a Daniel et al. 2019). Like early universe studies, standard candles are also useful to study the nature of dark energy (Wood-Vasey et al. 2007) which is still an open problem of cosmology (Davis et al. 2007 Davis Parkinson 2016).

In order to understand how H_0 value affects the measurements of dynamic dark energy EoS model parameters, we simply cross-correlated the data in tables 1 and 2. Figures 2 and 3 show how the measurement or choice of the Hubble Constant can affect the measurements of dynamic dark energy EoS parameters in WCDM and CPL models. We can clearly observe significant negative cross-correlation between w_0 and H_0 for both WCDM and CPL models.

These results are particularly interesting due to the Hubble Constant tension arising due to the differences in measurements of H_0 through cosmic microwave background, standard candles and other techniques.

Table 1: Best fit values for WCDM model using union

2.1 dataset				
WCDM				
H_0	$\Omega\Lambda$	w_0	χ^2	Bounds on $\Omega\Lambda, w_0$
67.400	0.75	-0.7024	606.6761	$(0.65, 0.75), (-\infty, -1/3)$
67.400	0.75	-0.7024	606.6761	$(0.65, 0.75), (-1, -1/3)$
73.520	0.65	-1.7459	614.5908	$(0.65, 0.75), (-\infty, -1/3)$
73.520	0.75	-1.0000	740.6163	$(0.65, 0.75), (-1, -1/3)$
70.000	0.72	-1.0045	562.2257	$(0.65, 0.75), (-\infty, -1/3)$
70.000	0.72	-1.0000	562.2267	$(0.65, 0.75), (-1, -1/3)$
72.500	0.65	-1.5683	588.7033	$(0.65, 0.75), (-\infty, -1/3)$
72.500	0.75	-1.0000	646.1989	$(0.65, 0.75), (-1, -1/3)$
67.770	0.75	-0.7353	594.2718	$(0.65, 0.75), (-\infty, -1/3)$
67.770	0.75	-0.7353	594.2718	$(0.65, 0.75), (-1, -1/3)$
69.185	0.75	-0.8645	565.9402	$(0.65, 0.75), (-\infty, -1/3)$
69.185	0.75	-0.8645	565.9402	$(0.65, 0.75), (-1, -1/3)$

Table 2: Best fit values for CPL model using union

2.1 dataset					
CPL					
H_0	$\Omega\Lambda$	w_0	w_a	χ^2	Bounds on $\Omega\Lambda, w_0, w_a$
66.300	0.65	-0.333	-3.601	620.9512	$(0.65, 0.75), (-\infty, -1/3), (-5, 5)$
66.300	0.65	-0.333	-3.601	620.9512	$(0.65, 0.75), (-1, -1/3), (-5, 5)$
66.300	0.75	-0.567	-0.300	650.2256	$(0.65, 0.75), (-\infty, -1/3), (-0.3, 0.3)$
66.300	0.75	-0.567	-0.300	650.2256	$(0.65, 0.75), (-1, -1/3), (-0.3, 0.3)$
67.400	0.65	-0.333	-4.678	585.7344	$(0.65, 0.75), (-\infty, -1/3), (-5, 5)$
67.400	0.65	-0.333	-4.678	585.7344	$(0.65, 0.75), (-1, -1/3), (-5, 5)$
67.400	0.75	-0.664	-0.300	602.6112	$(0.65, 0.75), (-\infty, -1/3), (-0.3, 0.3)$
67.400	0.75	-0.664	-0.300	602.6112	$(0.65, 0.75), (-1, -1/3), (-0.3, 0.3)$
67.770	0.65	-0.419	-4.326	579.2176	$(0.65, 0.75), (-\infty, -1/3), (-5, 5)$
67.770	0.65	-0.419	-4.326	579.2176	$(0.65, 0.75), (-1, -1/3), (-5, 5)$
67.770	0.75	-0.697	-0.300	590.9692	$(0.65, 0.75), (-\infty, -1/3), (-0.3, 0.3)$
67.770	0.75	-0.697	-0.300	590.9692	$(0.65, 0.75), (-1, -1/3), (-0.3, 0.3)$
68.340	0.65	-0.584	-3.491	571.3333	$(0.65, 0.75), (-\infty, -1/3), (-5, 5)$
68.340	0.65	-0.584	-3.491	571.3333	$(0.65, 0.75), (-1, -1/3), (-5, 5)$
68.340	0.75	-0.749	-0.300	577.1210	$(0.65, 0.75), (-\infty, -1/3), (-0.3, 0.3)$
68.340	0.75	-0.749	-0.300	577.1210	$(0.65, 0.75), (-1, -1/3), (-0.3, 0.3)$
69.185	0.65	-0.830	-2.278	564.2394	$(0.65, 0.75), (-\infty, -1/3), (-5, 5)$
69.185	0.65	-0.830	-2.278	564.2394	$(0.65, 0.75), (-1, -1/3), (-5, 5)$
69.185	0.75	-0.827	-0.300	565.2861	$(0.65, 0.75), (-\infty, -1/3), (-0.3, 0.3)$
69.185	0.75	-0.827	-0.300	565.2861	$(0.65, 0.75), (-1, -1/3), (-0.3, 0.3)$
70.000	0.72	-1.005	-0.011	562.2257	$(0.65, 0.75), (-\infty, -1/3), (-5, 5)$
70.000	0.72	-1.005	-0.011	562.2257	$(0.65, 0.75), (-\infty, -1/3), (-0.3, 0.3)$
70.000	0.72	-1.000	0.039	562.2260	$(0.65, 0.75), (-1, -1/3), (-5, 5)$
70.000	0.72	-1.000	0.039	562.2260	$(0.65, 0.75), (-1, -1/3), (-0.3, 0.3)$
72.500	0.67	-1.727	2.402	583.9811	$(0.65, 0.75), (-\infty, -1/3), (-5, 5)$
72.500	0.65	-1.598	0.300	587.6217	$(0.65, 0.75), (-\infty, -1/3), (-0.3, 0.3)$
72.500	0.75	-1.000	-1.142	623.7469	$(0.65, 0.75), (-1, -1/3), (-5, 5)$
72.500	0.75	-1.000	-0.300	635.4969	$(0.65, 0.75), (-1, -1/3), (-0.3, 0.3)$
73.520	0.65	-2.101	3.575	603.5328	$(0.65, 0.75), (-\infty, -1/3), (-5, 5)$
73.520	0.65	-1.773	0.300	613.0368	$(0.65, 0.75), (-\infty, -1/3), (-0.3, 0.3)$
73.520	0.75	-1.000	-1.950	682.8480	$(0.65, 0.75), (-1, -1/3), (-5, 5)$
73.520	0.75	-1.000	-0.300	722.6496	$(0.65, 0.75), (-1, -1/3), (-0.3, 0.3)$

6 Results

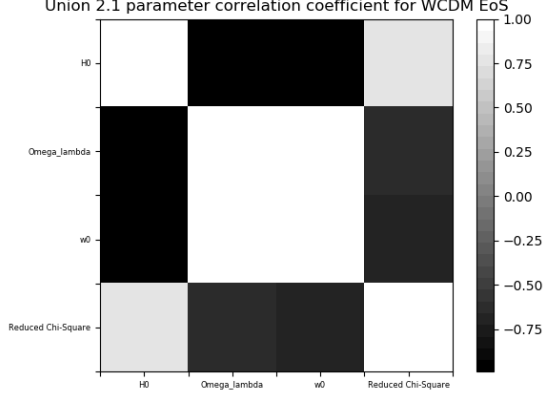


Figure 2: Cross-correlation of WCDM model parameters with H_0 , χ^2 and each other. We can clearly observe significant negative cross-correlation between w_0 and H_0 .

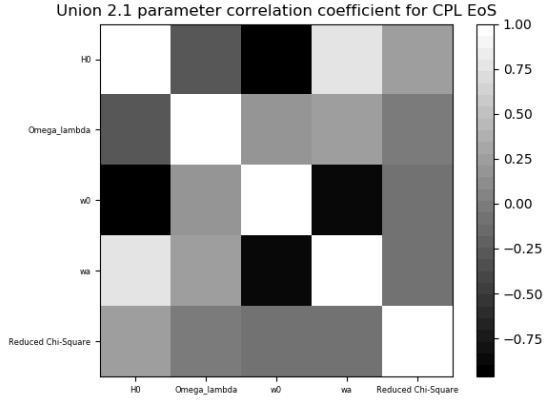


Figure 3: Cross-correlation of CPL model parameters with H_0 , χ^2 and each other. We can again clearly observe significant negative cross-correlation between w_0 and H_0 . We can also observe positive cross-correlation between H_0 and w_a .

In figure 4, for WCDM model, the maximum likelihood fit values are $\Omega\Lambda = 0.712^{+0.039}_{-0.021}$ and $w_0 = -0.995^{+0.070}_{-0.073}$. Their corresponding mean likelihood fit values are $\Omega\Lambda = 0.724 \pm 0.030$ and $w_0 = -1 \pm 0.065$. Both maximum and mean likelihood values agree, within one sigma overlapping values, with the best fit values obtained by using TRF and dog leg methods for $H_0=70$. The best values from tables 1 and 8 are $\Omega\Lambda = 0.720362 \pm 0.0626$ and $w_0 = -1.00449 \pm 0.1435$. Values in table 1 are rounded off to fit in the columns.

In figure 5, for CPL model, the maximum likelihood fit values are $\Omega\Lambda = 0.687^{+0.103}_{-0.060}$, $w_0 = -0.98^{+0.014}_{-0.014}$ and $w_a = -0.35^{+0.47}_{-0.92}$. Their corresponding mean likelihood fit values are $\Omega\Lambda = 0.731 \pm 0.080$, $w_0 = -1.02 \pm 0.015$ and $w_a = 0.01 \pm 0.65$. Again both maximum and mean likelihood values agree, within one sigma overlapping values, with the best fit values obtained by using TRF and dog leg methods for $H_0=70$. The best values from tables 2 and 8 are $\Omega\Lambda = 0.71933 \pm 0.27885$, $w_0 = -1.00547 \pm 0.291303$ and $w_a = -0.01126 \pm 3.033239$. Values in table 1 are rounded off to fit in the columns. For w_a , there is a relatively larger standard deviation in both likelihood estimates and in TRF and dog leg optimization approaches which is likely due to smaller redshift coverage from type Ia supernovae sample from Union 2.1. On very large redshifts, w_a almost plays an equal role as w_0 in CPL model because on extremely large 'z' values, $w_{de}(z)$ approximately becomes $w_0 + w_a$. However in case of a model like JBP, the model will be more or entirely dependent on w_0 . This means higher redshift surveys especially highly sensitive all sky surveys like galaxy surveys to study the late time integrated Sachs-Wolfe effect (ISW) (SachsWolfe 1967 Afshordi 2004 RahmanIqbal 2019) or surveys studying the early universe signatures like cosmic microwave background radiation (CMB) or baryonic acoustic oscillations (BAO), can play an important part in estimating parameters like w_a or other extended EoS model parameters can make major contributions in higher redshifts in various dynamic dark energy equation of state (EoS) models

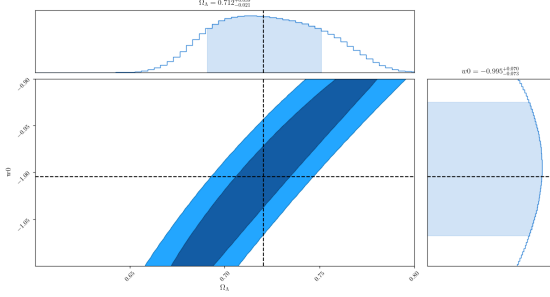


Figure 4: WCDM parameter constraints obtained through maximum likelihood and comparison with results from TRF and dog leg methods (dark dashed lines).

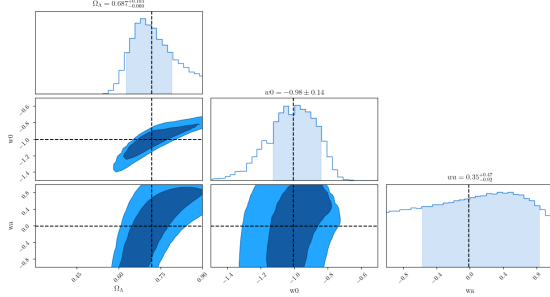


Figure 5: CPL parameter constraints obtained through maximum likelihood and comparison with results from TRF and dog leg methods (dark dashed lines).

which are in discussion in this study.

To see how dynamic dark energy EoS evolves in JBP, BA, PADE-I, PADE-II, and LH4 models especially in comparison the results from the flat Λ -CDM model with constant $w_{de}=-1$, WCDM and CPL models, we again applied TRF and dog leg methods (VoglislLagaris 2004) simultaneously and selected the best fit values based on χ^2 criteria.

We can see in figure 6 that for $H_0=70 \text{ km s}^{-1} \text{ Mpc}^{-1}$, the results are closer to Λ -CDM model with constant $w_{de}=-1$ except for BA model which is in quintessence regime and PADE-II which is a bit farther than $w_{de}=-1$ in comparison with others. However, due to large standard devia-

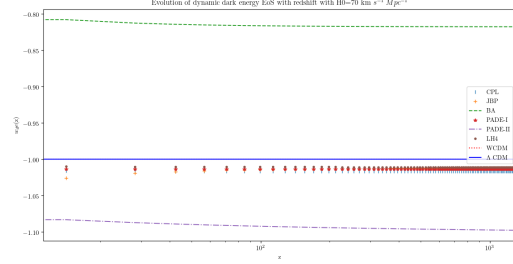


Figure 6: Evolution of $w_{de}(z)$ for various dynamic dark energy EoS models with redshift for $H_0=70 \text{ km s}^{-1} \text{ Mpc}^{-1}$.

tions from mean for w_a , w_b , a_t and T parameters in CPL, JBP,BA, PADE-I, PADE-II and LH4 models (BarbozaAlcaniz 2008ChevallierPolarski 2001Linder 2003 Jassal et al. 2005aJassal et al. 2005b LinderHuterer 2005 Wei et al. 2014) for relatively smaller redshift objects like in Union 2.1 dataset of type Ia supernovae, we still need to test these models using early universe signatures like CMB and BAO. For our type Ia supernova dataset with relatively smaller redshift coverage in comparison with they early universe studies, we can see that Λ -CDM model with $w_{de}=-1$ as fixed value is still the preferred model based on Bayesian information criterion (BIC) (Schwarz 1978Arevalo et al. 2017Liddle 2007) especially if we consider ΔBIC values which are basically the difference of BIC values from our models in discussion with the lowest BIC obtained from these models. $\Delta\text{BIC} > 2$ suggests positive evidence against a model with higher BIC and $\Delta\text{BIC} > 6$ suggests strong evidence against higher BIC value models (KassRaftery 1995) as BIC heavily penalizes the inclusion of newer parameters (Liddle 2007) despite having better χ^2 scores for non Λ -CDM models. This can change for higher redshift or early universe studies when extra parameters in dynamic dark energy EoS models are potentially going to play important role which will also be useful for H_0 studies (GorbunovRubakov 2011 Planck 2018Riess et al. 2019

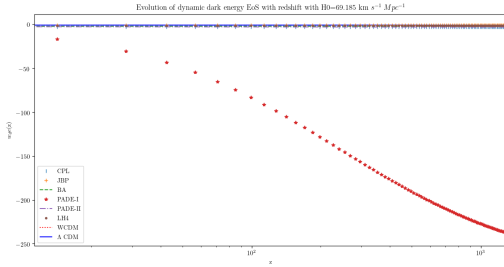


Figure 7: Evolution of $w_{de}(z)$ for various dynamic dark energy EoS models with redshift for $H_0=69.185 \text{ km s}^{-1} \text{ Mpc}^{-1}$.

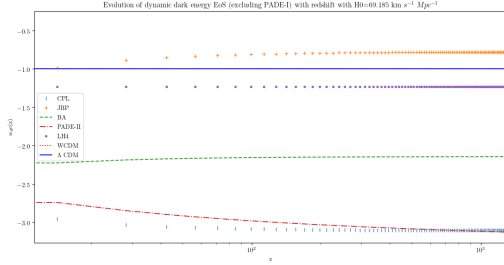


Figure 8: Evolution of $w_{de}(z)$ for various dynamic dark energy EoS models with redshift for $H_0=69.185 \text{ km s}^{-1} \text{ Mpc}^{-1}$ excluding PADE-I.

RisalitiLusso 2019Poulin et al. 2019Liu et al. 2019

For $H_0=69.185 \text{ km s}^{-1} \text{ Mpc}^{-1}$, we first look at figure 7 and observe that PADE-I is showing most deviation from $w_{de}=-1$ in comparison with the others especially at higher redshifts. This difference in scale of deviation towards $w_{de}=-1$ is due to the relatively higher contribution of w_a and w_b of PADE-I model with increasing redshift values. In figure 8, we remove PADE-I model to see the evolution of $w_{de}(z)$ in other models. We can see that apart from JBP, which is moving towards quintessence regime, others are closer to phantom regime (Vikman 2005Farnes 2018) with BA and PADE-II deviating away more from $w_{de}=-1$ and towards phantom regime. Theoretically, all structures

in our universe would be eventually ripped apart by the repulsive forced associated with the phantom dark energy (Vikman 2005Weinberg 2008). It will be interesting to see if future high precision standard candles, early universe and other surveys can settle expansion rate debate and which w_{de} evolution or best fit value will be associated with it as we can observe from figures 2 and 3 that expansion rate and dark energy EoS parameters have significant cross-correlation with each other.

We can also see from figures 6, 7 and 8 that despite H_0 values being $< 2\%$ different from each other, their impact on $w_{de}(z)$ evolution is significant for all the models. This difference is significant enough to impact our understanding of the scales and evolution of our universe which warrants the need to carefully model $w_{de}(z)$ in observations of early universe signatures, galaxy surveys, standard candles, standard rulers and recently discovered gravitational waves which can be used as standard sirens (Schutz 1999 Jarvis et al. 2014 Rahman 2018Chen et al. 2018). Gravitational waves can also be used to study the gravitational wave strain signals from type Ia supernovae and we can use them to study cosmological parameters. For this purpose it will be useful to carefully study the progenitors of the type Ia supernovae (KeiichiTerada 2016Rahman 2018) as the mass profiles of the objects involved will be crucial in modeling the expected signal (Schutz 1999Rahman 2018).

7 Conclusion

We studied various dynamic dark energy EoS models and also discussed the key EoS parameter w_0 in relation with the Hubble Constant. We also observed strong negative correlation between the Hubble Constant and EoS parameter w_0 . This relation is also studied in relation with different H_0 values obtained from various surveys adopting different techniques to constraint the cosmological parameters especially H_0 . We found that the models we tested agreed mostly with standard cosmological model predictions. We also observed that the extended dynamic dark en-

ergy equation of state (EoS) models we tested agreed with the idea of a universe going through an accelerated expansion phase. We also observed that the value of w_0 , which provides value of $w_{de}(z)$ at $z=0$ or the current epoch, is in quite close to the standard Λ -CDM constant value of $w_{de}=-1$ with $w_0=-1$ in the confidence interval of one sigma. For the Hubble Constant value of $H_0 \approx 69.185$, which we fit on Union 2.1 dataset using kinematic expression for luminosity distance, we found that best fit values for dynamic dark energy EoS models deviate from the constant $w_{de}=-1$. However, Λ -CDM with constant value of $w_{de}=-1$ still comes as the preferable model based on the BIC selection criteria. However this deviation, even in the EoS models with higher number of parameters, shows the importance of studying H_0 in relation with $w_{de}(z)$. Based on our results, we can also conclude that by carefully modeling and studying $w_{de}(z)$, we can potentially resolve the Hubble Constant tension arising from the results obtained using different techniques.

8 Acknowledgement

I would like to thank Prof. Dr. Jeremy Mould, Emeritus Professor at Swinburne University of Technology for reviewing this work and providing useful suggestions during the development of this paper.

Table 3. Best Fit Parameters for Dynamic Dark Energy EoS models using Union 2.1 SN type Ia Dataset

Hubble Constant H_0	EoS Models	Ω_m	Λ	w_0	Parameter Values	w_1	w_2	α_f	T	Chi-Square	Pars	BIC
70(Fixed)												
	Λ -CDM ($w, de=-1$)	0.722287 \pm 0.013		-1						562.2267	1	568.5897
	WCDM	0.720362 \pm 0.0626		-1.00449 \pm 0.1435						562.2257	2	574.9518
	CPL	0.71913 \pm 0.27885		-1.03547 \pm 0.291303	-0.01126 \pm 3.051239					562.2257	3	581.3144
	JBP	0.70796 \pm 0.17292		-1.011969 \pm 0.1643	-0.22393 \pm 3.2172					562.2219	3	581.311
	BA	0.75 \pm 0.86891		-0.9091 \pm 1.06464	0.15139 \pm 3.56007					562.2117	3	581.3008
	PADE-I	0.7196 \pm 1.24524		-1.00523 \pm 1.94515	-0.0078414 \pm 4.0909.4	-0.002752 \pm 4.882.5				562.2257	4	587.6778
	PADE-II	0.712676 \pm 0.4852		-1.01089 \pm 0.7073	1.10837 \pm 271.43	-0.998715 \pm 267.123				562.2249	4	582.6771
	LH4	0.72007 \pm 2.0615		-0.999102 \pm 223.47	-1.01078 \pm 314.32			0.9179244 \pm 29648.86	0.960383 \pm 39515.18	562.2258	5	594.0409
69.185(Fixed)												
	Λ -CDM ($w, de=-1$)	0.68671517 \pm 0.01366395		-1						567.9916	1	574.3146
	WCDM	0.75 \pm 0.08088		-0.86452 \pm 0.1448						565.9402	2	578.6663
	CPL	0.65 \pm 0.094414		-0.82971 \pm 0.112769	-2.27778 \pm 2.70177					564.2394	3	583.3285
	JBP	0.65 \pm 0.08967		-0.77572 \pm 0.13367	-3.38651 \pm 3.53197					563.8489	3	582.938
	BA	0.65 \pm 0.10223		-0.88266 \pm 0.1076	-1.260334 \pm 1.7368					564.787	3	582.796
	PADE-I	0.66386 \pm 0.12523		-0.88078055 \pm 0.11613	-0.299997 \pm 2.02684	-0.9958 \pm 0.0000003				564.1249	4	589.577
	PADE-II	0.65 \pm 0.2224		-0.81318 \pm 0.5637	3.440955 \pm 23.726	-0.999 \pm 20.04				564.1126	4	589.5647
	LH4	0.65596 \pm 0.05682		-0.38368 \pm 0.71809	-1.23068 \pm 0.28266			0.96887 \pm 0.03171	0.000875 \pm 0.26341	561.3035	5	593.1186

References

- [1] Abbott B.P. et al., 2016, Phys.Rev.Lett. 116 no.6, 061102 arXiv:1602.03837 [gr-qc] LIGO-P150914
- [2] Abott B. P. et al. , 2017, Phys.Rev.Lett. 119, 161101
- [3] Afshordi,2004, Phys. Rev. D,70,083536
- [4] Amanullah et al., 2010, (The Supernova Cosmology Project), Astrophys.J.716:712-738
- [5] Arevalo F., Cid A., Moya J., 2017, Eur. Phys. J. C 77: 565. <https://doi.org/10.1140/epjc/s10052-017-5128-7>
- [6] Barboza Jr. E. M. , Alcaniz J.S., 2008, Phys. Rev. B 666 415
- [7] Bennett C. L. et al., 2013, The Astrophysical Journal Supplement, Volume 208, Issue 2, article id. 20, 54 pp.
- [8] Birrer S, Treu T, Rusu C. E, et al., 2018, Monthly Notices of the Royal Astronomical Society. 484 (4): 4726–4753.
- [9] Chen Hsin-Yu, Fishbach Maya, Holz Daniel E., 2018, Nature, Volume 562, Issue 7728, p.545-547
- [10] Chevallier M, Polarski D, 2001, Int. J. Mod. Phys. D 10, 213, [gr-qc/0009008
- [11] Daniel S., Perlmutter S. et al., 2019, Astro2020: Decadal Survey on Astronomy and Astrophysics, science white papers, no. 270, arXiv:1903.05128
- [12] Davis T.M., Parkinson D., 2016, Characterizing Dark Energy Through Supernovae. In: Alsabti A., Murdin P. (eds) Handbook of Supernovae. Springer, doi:10.1007/978-3-319-20794-0_106-1
- [13] Davis T.M., Mörtsell E., ESSENCE et al., 2007, The Astrophysical Journal, Volume 666, Issue 2, pp. 716-725., astro-ph/0701510
- [14] Farnes J. S., 2018, Astronomy and Astrophysics. 620: A92
- [15] Freedman Wendy L., 2017, Nature Astronomy, Volume 1, id. 0121
- [16] Gorbunov S., Rubakov V.A. , 2011, Introduction to the Theory of the Early Universe: Cosmological Perturbations and Inflationary Theory, World Scientific, Singapore
- [17] Grieb Jan N., Sanchez Ariel G., Salazar-Albornoz Salvador, 2017, Monthly Notices of the Royal Astronomical Society, Volume 467, Issue 2, p.2085-2112
- [18] Hinshaw G. et al., 2013, Astrophys. J. Suppl. Ser., 208, 19
- [19] Jackson N., 2015, Living Rev Relativ 18: 2. <https://doi.org/10.1007/lrr-2015-2>
- [20] Jarvis M., Bacon D., Blake C. et al., 2014, SKA Cosmology Chapter, Advancing Astrophysics with the SKA (AASKA14) Conference, Giardini Naxos (Italy), June 9th-13th 2014, arXiv:1501.03825
- [21] Jassal H.K., Bagla J.S., Padmanabhan T., 2005, MNRAS 356 L11
- [22] Jassal H.K., Bagla J.S., Padmanabhan T., 2005b, Phys. Rev. D 72 103503
- [23] Jones E, Oliphant E, Peterson P, et al., 2001, <http://www.scipy.org/>
- [24] Kass Robert E., Raftery Adrian E., 1995, Journal of the American Statistical Association, 90 (430): 773–795, doi:10.2307/2291091, ISSN 0162-1459, JSTOR 2291091
- [25] Keiichi Maeda, Yukikatsu Terada, 2016, International Journal of Modern Physics D, Vol. 25, No. 10 1630024
- [26] Khosravi Nima, Baghran Shant, Afshordi Niayesh, Altamirano Natacha, 2019, Physical Review D, Volume 99, Issue 10, id.103526
- [27] Liddle A., 2003, "Introduction to modern Cosmology", Second edition, University of Sussex, UK, Wiley Publication

- [28] Liddle A.R., 2007, Monthly Notices of the Royal Astronomical Society: Letters, Volume 377, Issue 1, pp. L74-L78
- [29] The LIGO Scientific Collaboration, The Virgo Collaboration, The 1M2H Collaboration, The Dark Energy Camera GW-EM Collaboration and the DES Collaboration, The DLT40 Collaboration, The Las Cumbres Observatory Collaboration, The VINROUGE Collaboration, The MASTER Collaboration, Abbott et al., 2017, Nature. advance online publication (7678): 85–88. arXiv:1710.05835
- [30] Linder E. V., Huterer D., 2005, Phys. Rev. D 72, 043509
- [31] Linder E. V., 2003, Phys. Rev. Lett., 90, 091301, [astro-ph/0311403]
- [32] Bin Liu, Zhengxiang Li, Zong-Hong Zhu, 2019, Monthly Notices of the Royal Astronomical Society, Volume 487, Issue 2, Pages 1980–1985, <https://doi.org/10.1093/mnras/stz1179>
- [33] Macaulay E., Nichol R. C., Bacon D. et al., 2019, Monthly Notices of the Royal Astronomical Society, Volume 486, Issue 2, Pages 2184–2196, <https://doi.org/10.1093/mnras/stz978>
- [34] Perlmutter S., Schmidt B., 2003, Supernovae and Gamma Ray Bursters, K. Weiler, ed., Springer-Verlag, New York
- [35] Perlmutter S., 1999, Astrophys. J. 517, 565
- [36] Pietrzyński G., Graczyk D., Galenne A., et al. 2019, Nature, 567, 200. <https://doi.org/10.1038/s41586-019-0999-4>
- [37] Planck Collaboration, Bucher, P. A. R. et al., 2014, A&A 571: A1
- [38] Planck Collaboration, P.A.R. Ade, et al., 2014, A&A, Volume 571, id.A23, 48 pp.
- [39] Planck Collaboration, 2016, A&A 594, A1
- [40] Planck Collaboration, 2018, www.cosmos.esa.int. arXiv:1807.06209
- [41] Poulin Vivian, Smith Tristan L., Karwal Tanvi, Kamionkowski Marc, 2019, Physical Review Letters, Volume 122, Issue 22, id.221301
- [42] Rahman S.F., Iqbal M.J., 2019, Eur. Phys. J. Plus 134: 302. <https://doi.org/10.1140/epjp/i2019-12669-y>
- [43] Rahman S.F. Astronomy & Geophysics, Volume 59, Issue 2, Pages 2.39–2.42, 2018
- [44] Riess et al., 1998, AJ Vol. 16
- [45] Riess et al., 2007, Astrophys. J. 659 98-121 [astro-ph/0611572 46455850950](https://doi.org/10.1086/518645)
- [46] Riess A. G., Macri L. M., Hoffmann S. L., et al. 2016, ApJ, 826, 56
- [47] Riess et al., 2018, The Astrophysical Journal, Volume 853, Issue 2, article id. 126, 15 pp.
- [48] Riess Adam G., Casertano Stefano, Yuan Wenlong et al., 2018, The Astrophysical Journal. 861 (2): 126
- [49] Riess Adam G., Casertano Stefano, Yuan Wenlong, Macri Lucas M., Scolnic, Dan, 2019, arXiv:1903.07603, ApJ accepted 2019
- [50] Risaliti G., Lusso E., 2019, Nature Astronomy volume 3, pages 272-277
- [51] Sachs R.K., 1967, Wolfe A.M., Astrophys. J., 147, 73
- [52] Sandage A. R., 1958, Astrophysical Journal, vol. 127, p.513
- [53] Classical and Quantum Gravity, Volume 16, Number 12A
- [54] Schwarz Gideon E., 1978, Annals of Statistics, 6 (2): 461–464, doi:10.1214/aos/1176344136
- [55] Solà Peracaula Joan, Gázquez-Valent Adrià, de Cruz Pérez Javier, 2019, Physics of the Dark Universe, Volume 25, article id. 100311.
- [56] Soltis J., Farahi A., Huterer D., Liberato C.M., 2019, Phys. Rev. Lett. 122, 091301

- [57] Suzuki et al., 2012 (The Supernova Cosmology Project), The Astrophysical Journal, Volume 746, Issue 1, article id. 85, 24 pp.
- [58] Vattis Kyriakos, Koushiappas Savvas M., Loeb Abraham, 2019, Physical Review D, Volume 99, Issue 12, id.121302
- [59] Vikman Alexander, 2005, Phys. Rev. D. 71 (2): 023515
- [60] Voglis C., Lagaris I.E., 2004, WSEAS International Conference on Applied Mathematics, Corfu, Greece
- [61] Watson D., Denney K.D. et al., 2011, ApJ 740, L49
- [62] Wei H., Yan X.P., Zhou Y.N., 2014, JCAP 1401, 045, 1312.1117
- [63] Weinberg Steven, 2008, "Cosmology", Oxford University Press, ISBN 0191523607, 9780191523601
- [64] Wojtak Radosław, Agnello Adriano, 2019, Monthly Notices of the Royal Astronomical Society, Volume 486, Issue 4, p.5046-5051
- [65] Wood-Vasey et al., 2007, Astrophys.J.666:694-715, arXiv: astro-ph/0701041
- [66] Zhai A., Blanton M., Slosar A., Tinker J., 2017, The Astrophysical Journal, Volume 850, Issue 2, article id. 183, 32 pp.